SLAC–PUB–6034
January 1993
(E/T)

First Measurement of the Left-Right Z Cross Section Asymmetry in Polarized e^+e^- Collisions at the SLC*

THE SLD COLLABORATION

represented by

MORRIS L. SWARTZ

Stanford Linear Accelerator Center
Stanford University, Stanford, California, 94309

ABSTRACT

The SLAC Linear Collider (SLC) has recently been upgraded to produce, accelerate, and collide a spin polarized electron beam. The average beam polarization during the 1992 run was (22.4±0.7)%. The SLD Collaboration used the polarized beam to perform the first measurement of the left-right cross section asymmetry (A_{LR}) for Z boson production by e^+e^- collisions. The measurement was performed at a center-of-mass energy of 91.55 GeV with a sample of 10,224 Z decays. The measured value of A_{LR} is 0.100±0.044(stat.)±0.004(syst.) which determines the effective weak mixing angle to be $\sin^2\theta_W^{\text{eff}} = 0.2378 \pm 0.0056(\text{stat.}) \pm 0.0005(\text{syst.})$.

Invited talk presented at the 10th International Symposium
on High Energy Spin Physics, Nagoya, Japan
November 9-14, 1992

⋆ Work supported by the Department of Energy, contract DE–AC03–76SF00515.

1. The Polarized SLC

The SLAC Linear Collider (SLC) has recently been upgraded to produce, accelerate, and collide a spin-polarized electron beam.[1] A diagram of the SLC is shown in Figure 1.

The 120 KV polarized electron source was described in great detail in the Polarized Electron Source Workshop.[2,3] Longitudinally polarized electrons are produced by photoemission from a gallium arsenide cathode which is illuminated by a circularly polarized laser beam of wavelength $\lambda = 715$ nm. During each SLC machine cycle (the SLC operates at 120 Hz), the polarized electron source produces two pulses of approximately 6×10^{10} electrons of 2 ns duration (full width at half maximum) separated by 61 ns.[4] The quantum efficiency of the photocathode ranged from 3% to 8%. The instantaneous current produced by the SLC polarized electron source was limited by a newly discovered *charge-limit effect*[5] which required that the quantum efficiency be maintained at a level above 3%. This in turn required that the cathode be recesiated about once per week and that it be reactivated approximately once per month. The downtime of the source was dominated by this maintenance schedule and was 7%. The polarization of the emitted electrons is 28-29%.[6] The electron helicity is changed randomly on a cycle-by-cycle basis by changing the circular polarization of the laser beam.

The pair of electron pulses is accelerated to 1.16 GeV and stored in the North Damping Ring of the SLC. A system composed of the dipole magnets of the Linac-To-Ring (LTR) transfer line and a superconducting solenoid magnet is used to rotate the longitudinal polarization of the beam into the vertical direction for storage in the damping ring. A system composed of two superconducting solenoids and the dipole magnets of the Ring-To-Linac transfer line is used to reorient the polarization vector upon extraction from the damping ring. This system has the ability to provide nearly all polarization orientations in the linac.

The LTR spin rotation system was designed to operate at the damping design energy of 1.21 GeV. Since the damping ring is currently operated at 1.16 GeV, the net spin precession in the LTR dipole magnets is less than the 90° design value. The resulting polarization direction of the electron beam at injection into the damping ring is not perfectly aligned with the vertical magnetic guide fields and some depolarization results. The spin transmission of the system is 0.95.

The leading electron pulse is accelerated in the linac to 46.7 GeV. The trailing pulse is accelerated to 30 GeV and is used to produce positrons for the next SLC cycle.[7] The leading pulse is then transported through the North Arc and Final Focus systems of the SLC to the interaction point (IP) of the machine. The North Arc is composed of 23 achromats, each of which consists of 20 combined function magnets. Each achromat causes 1085° of spin precession and 1080° of betatron phase advance. The arc therefore operates near a spin resonance. Due to the short length of the arc, this resonance does not strongly depolarize the beam but does cause the net spin rotation of the arc to depend upon the details of the actual orbit that is used. In particular, the spin precessions caused by each half of a vertical betatron oscillation may reinforce each other rather than cancel if the initial spin direction is unfavorably phased with the oscillation. This effect vanishes as the amplitude of the oscillation vanishes and can become significant for oscillation amplitudes as small as 50 μm. Unfortunately, we do not have sufficient knowledge of the absolute arc orbit to accurately predict the net spin precession of the system. The solution is to empirically measure the net precession of the arc by measuring the longitudinal polarization at the interaction point for three orthogonal spin directions in the linac. This determines two net rotation angles and the norm of the polarization vector. Since the net rotation is sensitive to variations in the arc orbit, a fast feedback loop was implemented to stabilize the launch of the electron bunch into the arc.

The transport of the beam through the North Arc causes some depolarization. The net spin rotation of the arc is energy dependent and the presence of a finite beam energy spread (0.3%) causes a spread in the orientations of the electron spin vectors at the interaction point. Simulations show that this effect can be enhanced by vertical betatron oscillations. Simlarly, arc orbit variations can cause an effective depolarization due to incorrect compensation of the net rotation. The effects resulted in a typical net spin transmission of 0.85.

After passing through the interaction point, the electron beam polarization is measured with the Compton polarimeter. The electron and positron beams are then transported to the south and north beam dumps, respectively. The mean e^+e^- center-of-mass energy during polarized operation was $E_{cm} = 91.55 \pm 0.04$ GeV[8].

2. The Polarization Measurement

The longitudinal beam polarization ($\mathcal{P}_e$) is measured by a Compton scattering polarimeter[9] located 33 m downstream of the IP. After it has passed through the IP and before it is deflected by dipole magnets, the electron beam collides with a circularly polarized photon beam produced by a frequency-doubled Nd:YAG laser of wavelength 532 nm. The scattered and unscattered electron beams remain unseparated until they pass through a pair of dipole magnets. The scattered electrons are dispersed horizontally and exit the vacuum system through a thin window. Multichannel Cherenkov and proportional tube detectors measure the momentum spectrum of the electrons in the interval from 17 to 30 GeV/c. The polarization of the laser beam ($\mathcal{P}_\gamma$) is measured to be (93±2)% and the sign of the circular polarization is changed randomly on sequential laser pulses.

The counting rates in each detector channel are measured for parallel and antiparallel combinations of the photon and electron beam helicities. The asymmetry formed from these rates is equal to the product $\mathcal{P}_e\mathcal{P}_\gamma A(E)$ where $A(E)$ is the theoretical asymmetry function at the accepted energy E of the scattered electrons.[10] The channel-by-channel polarization asymmetry, averaged over a large fraction of the data sample, is shown as a function of the mean channel position in Figure 2. The curve represents the product of $A(E)$ and a normalization factor ($\mathcal{P}_e\mathcal{P}_\gamma$) that has been adjusted to achieve a best fit to the measurements. The overall detector position and the momentum scale of the spectrometer are calibrated from measurements of the kinematic endpoint and the zero-asymmetry point.

Polarimeter data are acquired continually for runs of approximately 3 minutes. For each run, $\mathcal{P}_e$ is determined from the observed asymmetry using the measured value of $\mathcal{P}_\gamma$ and the theoretical asymmetry function. The absolute statistical precision of each run is typically $\delta\mathcal{P}_e = 0.8\%$. The systematic uncertainties that affect the polarization measurement are summarized in Table 1. The total relative systematic uncertainty is estimated to be $\delta\mathcal{P}_e/\mathcal{P}_e = 2.7\%$.

Table 1. Systematic uncertainties that affect the polarization measurement.

Systematic Uncertainty	$\delta\mathcal{P}_e/\mathcal{P}_e$
Laser Polarization	2.0%
Detector Linearity	1.5%
Interchannel Consistency	0.9%
Spectrometer Calibration	0.4%
Electronic Noise Correction	0.4%
Total Uncertainty	2.7%

The polarimeter measures the electron scattering rate for two helicity states of electrons and two helicity states of photons. Two non-zero asymmetries and two null asymmetries are formed from the measured scattering rates. The non-zero asymmetries determine the average polarizations of the left- and right-handed beams to be 22.00±0.02% and 22.13±0.02%, respectively. The two false polarizations that are determined from the null asymmetries are small as compared with the systematic error.

An additional systematic error would arise if the average beam polarization at the electron-photon crossing point differed from the luminosity-weighted average beam polarization at the SLC IP. We have investigated phase space and beam transport effects, depolarization caused by beam-beam interactions at the IP,[11] and an effect caused by the possible systematic deviation of the luminosity-weighted mean beam energy from the average beam energy.[12] All of these effects cause fractional polarization differences that are smaller than 0.1%.

3. The A_{LR} Measurement

The left-right asymmetry is defined as,[13]

$$A_{LR} \equiv (\sigma_L - \sigma_R) \,/\, (\sigma_L + \sigma_R)\,, \tag{1}$$

where σ_L and σ_R are the e^+e^- production cross sections for Z bosons (at the Z pole) with left-handed and right-handed electrons, respectively. To leading order, the Standard Model predicts that this quantity depends upon the vector (v_e) and axial-vector (a_e) couplings of the Z boson to the electron current,

$$A_{LR} = \frac{2 v_e a_e}{v_e^2 + a_e^2} = \frac{2\left[1 - 4\sin^2\theta_W^{\text{eff}}\right]}{1 + \left[1 - 4\sin^2\theta_W^{\text{eff}}\right]^2}, \tag{2}$$

where the effective electroweak mixing parameter is defined as $\sin^2\theta_W^{\text{eff}} \equiv (1 - v_e/a_e)/4$.[14] Note that A_{LR} has the following properties: it is a sensitive function of $\sin^2\theta_W^{\text{eff}}$, it is expected to be large (0.10-0.15), and it does not depend upon the couplings of the Z to its final states.

The left-right asymmetry is measured by counting hadronic and $\tau^+\tau^-$ decays of the Z boson for each of the two longitudinal polarization states of the electron beam. The measurement requires knowledge of the absolute beam polarization, but does not require knowledge of the absolute luminosity, detector acceptance, or efficiency.[15]

The polarized e^+e^- collisions are measured by the SLD detector which has been described elsewhere.[16] For this measurement, the triggering of the SLD and the selection of Z events were based solely upon calorimetry. The liquid argon calorimeter (LAC),[17] which covers 98% of the full solid angle, is segmented in depth into two electromagnetic sections (21 radiation length thickness) and two hadronic sections (2.8 interaction length thickness for the entire LAC), each of which is transversely segmented into projective towers of constant solid angle (there are approximately 17,000 towers in the first electromagnetic section). The calorimetric analysis must distinguish Z events from several backgrounds that are unique to the operation of a linear collider and differ from those encountered at e^+e^- storage rings. The backgrounds fall into two major categories: those due to low energy electrons and photons that scatter from various beamline elements and apertures, and those due to high energy muons that traverse the detector parallel to the beam axis (due to the low average current in the SLC, backgrounds caused by beam collisions with residual gas in the beamline are negligible). The beam-related backgrounds in the calorimeters are characterized by small amounts of energy in a large number of towers parallel to the beam direction. In order to suppress these backgrounds, all towers used in the analysis are required to satisfy a combination of threshold cuts and criteria that select against longitudinally localized energy deposition in a combined electromagnetic-hadronic tower. Each candidate event must contain fewer than 3000 accepted towers (of the 40,000 total) and the total energy observed in the endcap region of the warm iron calorimeter,[18] where beam backgrounds are large, must be less than 12 GeV. All events are required to have at least 20 GeV in the LAC and to be energy balanced.

The combined efficiency of the trigger and selection criteria is estimated to be (90±2)% for hadronic Z decays and about 30% for tau pairs. Because the event selection is calorimeter based, muon pairs are not included in the sample. Comparing this selection procedure with one that is based upon charged particle tracking information, and by applying the selection procedure to Monte Carlo events, we estimate that the residual beam-related background in the Z sample is less than 0.7%. The contribution of two-photon processes to the Z sample has been estimated by a Monte Carlo simulation to be less than 0.1%. Final state e^+e^- events are explicitly removed since the presence of the t-channel photon exchange subprocess dilutes the value of A_{LR}. We apply an e^+e^- identification procedure which searches for large and highly localized energy deposition in the electromagnetic section of the LAC. The residual e^+e^- background in the Z sample is estimated to be approximately 0.7%.

The sign of the electron beam helicity is supplied to the SLD data acquisition system via two redundant data paths. The synchronization of the helicity signals with triggered and logged events was verified on several occasions.

A total of 10,224 Z events satisfy the selection criteria. We find that 5,226 (N_L) of the events were produced with the left-handed electron beam and 4,998 (N_R) were produced with the right-handed beam.[19] The measured left-right cross section asymmetry for Z production is defined as

$$A_{LR}^{meas} \equiv (N_L - N_R)/(N_L + N_R) = (2.23 \pm 0.99) \times 10^{-2}.$$

The measured asymmetry A_{LR}^{meas} is related to A_{LR} by the following expression which is accurate to lowest order in the correction terms,

$$A_{LR} = \frac{1}{\mathcal{P}_e}\left[A_{LR}^{meas}(1+f_b) + (A_{LR}^{meas})^2 A_{\mathcal{P}} - E_{cm}\frac{\sigma'(E_{cm})}{\sigma(E_{cm})}A_E - A_\varepsilon - A_{\mathcal{L}}\right], \quad (3)$$

where $\mathcal{P}_e$ is the luminosity-weighted average beam polarization; f_b is the background fraction; $\sigma(E)$ is the unpolarized Z cross section at energy E; $\sigma'(E)$ is the derivative of the cross section with respect to E; and $A_{\mathcal{P}}$, A_E, A_ε, and $A_{\mathcal{L}}$ are the left-right asymmetries of the beam polarization, the center-of-mass energy, the product of detector acceptance and efficiency, and the integrated luminosity.

The correction to A_{LR}^{meas} for background contamination is less than 3.1×10^{-4}. The polarization asymmetry is directly measured to be $A_{\mathcal{P}} = -2.9 \times 10^{-3}$, resulting in a negligible correction. A left-right beam energy asymmetry would arise primarily from a left-right beam current asymmetry via beam-loading of the accelerator. Using the measured left-right current asymmetry, we infer that the A_E correction to A_{LR}^{meas} is $(1.7\pm0.6)\times10^{-5}$. The SLD has a symmetric acceptance in polar angle[15] which implies that the efficiency asymmetry A_ε is negligible.

A significant left-right luminosity asymmetry could be produced only by an asymmetry in the beams emitted by the polarized electron source. Such effects are expected to be quite small.[3] We verify this by examining a sample of 25,615 small-angle Bhabha scattering events detected by the luminosity monitoring system (LUM).[20] Of these, 12,832 events were produced with the left-handed electron beam and 12,783 were produced with the right-handed beam. Since the left-right cross section asymmetry for small-angle Bhabha scattering is expected to be small ($\sim 3\times10^{-4}\mathcal{P}_e$ in the LUM acceptance), the left-right asymmetry formed from the luminosity Bhabha events is a direct measure of $A_{\mathcal{L}}$. We measure $A_{\mathcal{L}}$ to be $(1.9\pm6.2)\times10^{-3}$. A more precise determination of $A_{\mathcal{L}}$ follows from a study of the three parameters of the electron beam (all defined at the IP) that determine the SLC luminosity: the beam current, the electron-positron beam offset, and the beam size (the beam is approximately round). The first two quantities are measured directly. The beam size is not measured directly but can be inferred from the flux of beamstrahlung photons produced by beam-beam interactions at the interaction point. By measuring the left-right asymmetries of each of these quantities, we conclude that $A_{\mathcal{L}}$ is $(1.8\pm4.2)\times10^{-4}$.

Since all corrections listed in equation (3) are consistent with zero or are extremely small, we do not apply them to A_{LR}^{meas} but include them in the systematic uncertainty on A_{LR}. Equation (3) then takes the following simple form,

$$A_{LR} = \frac{A_m}{\mathcal{P}_e} = \frac{1}{\mathcal{P}_e}\left(\frac{N_L - N_R}{N_L + N_R}\right). \tag{4}$$

Because $A_{\mathcal{L}}$ is small, the luminosity-weighted average polarization can be estimated from measurements of the beam polarization made when valid Z events are recorded,

$$\mathcal{P}_e = \frac{1}{N_Z}\sum_{i=1}^{N_Z}\mathcal{P}_i = (22.4 \pm 0.7)\%, \tag{5}$$

where N_Z is the total number of Z events, and $\mathcal{P}_i$ is the polarization measurement associated in time with the i^{th} event. The error on $\mathcal{P}_e$ is dominated by the systematic uncertainty on the polarization measurement.

Using equation (4), we find the left-right asymmetry to be

$$A_{LR} = 0.100 \pm 0.044(\text{stat.}) \pm 0.004(\text{syst.}),$$

where the systematic error has contributions from the uncertainties on $\mathcal{P}_e$, $A_{\mathcal{L}}$, and f_b. We use this measurement to derive the following value for the effective electroweak mixing parameter,

$$\sin^2\theta_W^{\text{eff}} = 0.2378 \pm 0.0056(\text{stat.}) \pm 0.0005(\text{syst.}),$$

where we have corrected the result to account for the deviation of the SLC center-of-mass energy from the Z-pole energy and for initial state radiation.[21] These results are consistent with recent measurements of τ polarization and the leptonic forward-backward asymmetries made by other experiments[22] and demonstrate the utility of a new, statistically powerful, and systematically precise technique for testing the Standard Model.

REFERENCES

1. For more details, see K. Moffeit, SLAC-PUB-6005, November 1992.
2. The SLC polarized electron gun is described in D. Schultz *et al.*, SLAC-PUB-5768, March 1992.
3. The SLC polarized light source is described in M. Woods *et al.*, SLAC-PUB-5965, December 1992.
4. Transmission losses reduce the beam pulses to 3×10^{10} electrons downstream of the damping ring.
5. M. Woods *et al.*, SLAC-PUB-6019, December 1992.
6. The electron polarization at the source is inferred from laboratory measurements of an identical cathode. This value is consistent with polarization measurements made with the Møller polarimeter at the end of the linac.
7. The collected positrons have energies in the range 2-20 MeV. Therefore, the positrons are not expected to retain any of the incident electron polarization. Even if this were not true, the arrival of a positron bunch at the SLC interaction point is delayed by one machine cycle with respect to its production electron bunch. The use of random electron beam helicity reversal insures that the helicities of the electron and positron bunches are uncorrelated.
8. The SLC energy is determined with energy spectrometers which are described in J. Kent *et al.*, SLAC-PUB-4922, March 1989.
9. The Compton Polarimeter is described in the presentation of M. Fero in these proceedings.
10. See S.B. Gunst and L.A. Page, *Phys. Rev.* **92**, 970 (1953) or H.A. Olsen, *Applications of QED*, Springer Tracts in Modern Physics, Vol. 44, p.83, (1968).
11. K. Yokoya and P. Chen, SLAC-PUB-4692, September 1988.

12. See Reference 8 and G.S. Abrams *et al.*, *Phys. Rev. Lett.*, **63**, 2173 (1989).

13. A review of the properties of A_{LR} can be found in D.C. Kennedy *et al.*, *Nuc. Phys.* **B321**, 83 (1989).

14. We follow the convention used by the LEP Collaborations in *Phys. Lett.* **B276**, 247 (1992).

15. The value of A_{LR} is unaffected by decay-mode-dependent variations in detector acceptance and efficiency provided that the efficiency for detecting a fermion at some polar angle (with respect to the electron direction) is equal to the efficiency for detecting an antifermion at the same polar angle. The SLD has an azimuthally symmetric solenoidal magnetic field which ensures the equality of particle and antiparticle efficiencies even in the presence of detector nonuniformities. Additionally, the SLD calorimeter has a high degree of uniformity and polar symmetry.

16. The SLD Design Report, SLAC Report 273, 1984.

17. D. Axen *et al.*, SLAC-PUB-5354, January 1990 (to be published in Nucl. Inst. Meth. A).

18. A.C. Benvenuti *et al.*, SLAC-PUB-5713, January 1992.

19. The sign of the beam helicity is inferred from the sign of the measured Compton scattering asymmetry, the measured helicity of the polarimeter laser, and the theoretical sign of the Compton scattering asymmetry (S. Drell and M. Peskin, private communication).

20. S.C. Berridge *et al.*, *IEEE Trans. Nucl. Sci.* **NS-39**, 242 (1992).

21. The correction from the result given by equation 14 is +0.0003. Our calculation agrees with the results given by the EXPOSTAR program described in D.C. Kennedy *et al.*, *Z. Phys.* **C53**, 617 (1992), and a modified version of the ZSHAPE program described in W. Beenakker, *et al.*, CERN-TH-5468-89, July 1989.

22. ALEPH Collaboration: D. Decamp *et al.*, *Z. Phys.* **C53**, 1 (1991) and *Phys. Lett.* **B265**, 430 (1991); DELPHI Collaboration: P. Aarnio *et al.*, *Nucl. Phys.* **B367**, 511 (1992) and P. Abreu *et al.*, *Z. Phys.* **C55**, 555 (1992); L3 Collaboration: B. Adeva *et al.*, *Z. Phys.* **C51**, 179 (1991) and O. Adriani *et al.*, *Phys. Lett.* **B294**, 466 (1992); OPAL Collaboration: G. Alexander *et al.*, *Z. Phys.* **C52**, 175 (1991) and *Phys. Lett.* **B266**, 201 (1991).

FIGURE CAPTIONS

1) The polarized SLC. The electron spin direction is indicated by the double-arrow.

2) The average polarized Compton scattering asymmetry as measured by seven channels of the Cherenkov detector is plotted as a function of the distance (d) from the trajectory of the undeflected beam. The curve represents the product of the asymmetry function and a normalization factor that has been adjusted to achieve a best fit to the measurements.

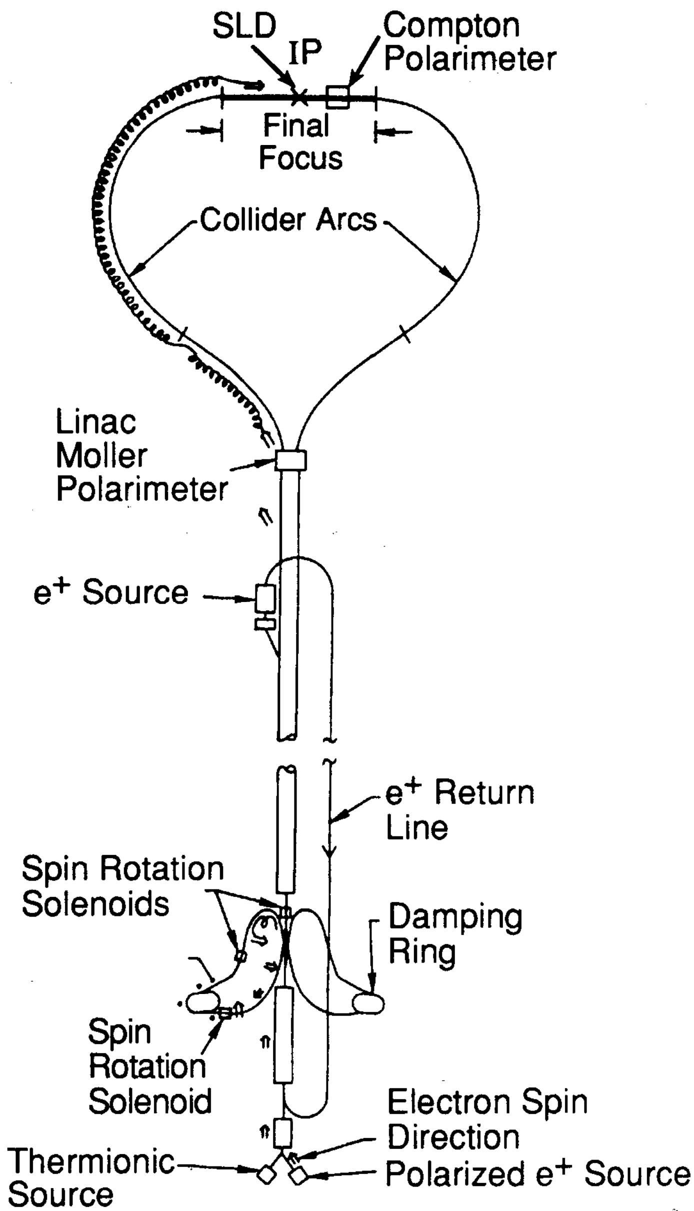

POLARIZATION IN THE OVERALL SLC LAYOUT

9-92 7220A5

Fig. 1

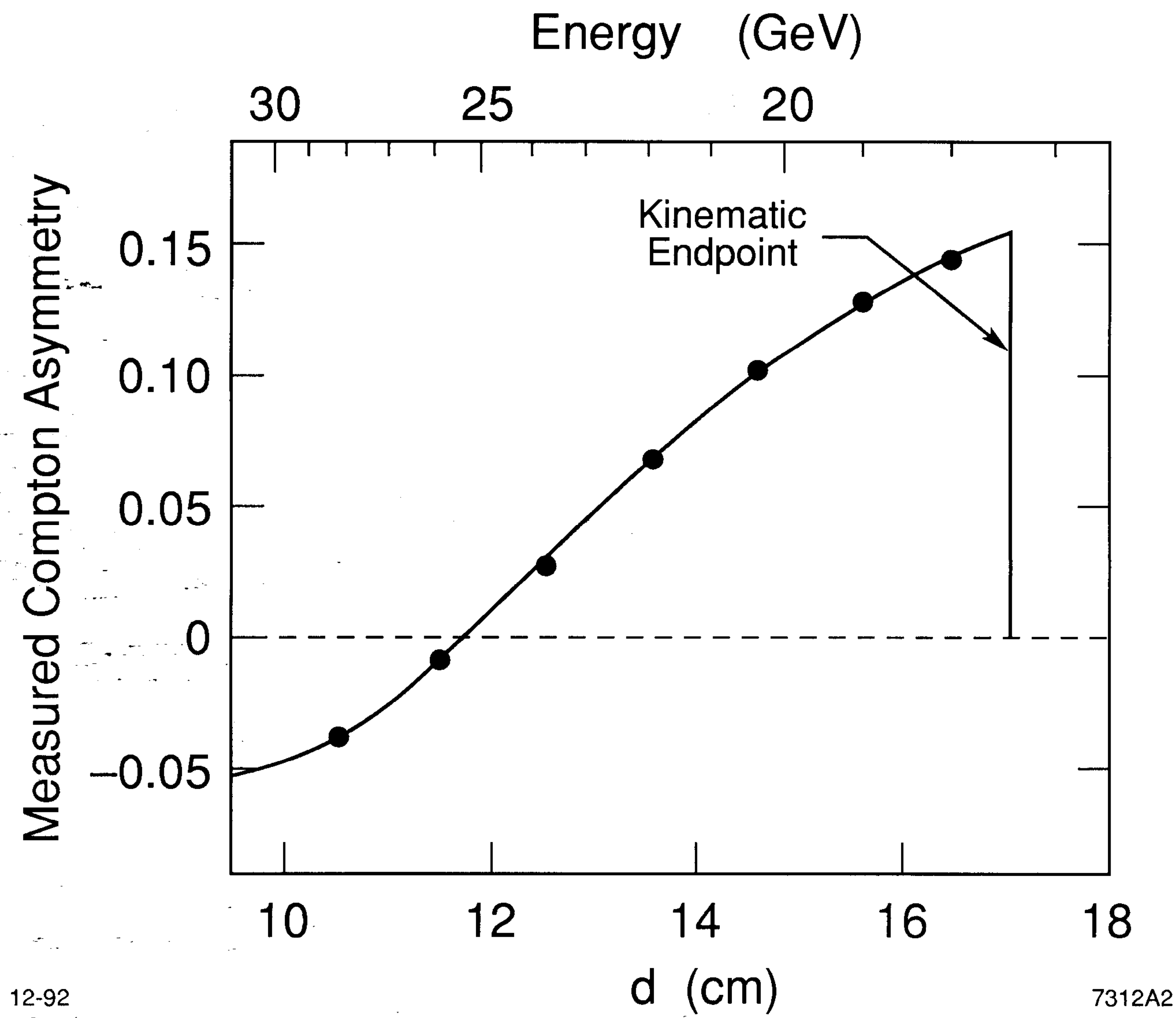

Energy (GeV)
30
25
20
Kinematic
Endpoint
Measured Compton Asymmetry
0.15
0.10
0.05
0
–0.05
10
12
14
16
18
d (cm)
12-92
7312A2

Fig. 2